Cancer Research

# Multivalent Forms of the Notch Ligand DLL-1 Enhance Antitumor T-cell Immunity in Lung Cancer and Improve Efficacy of EGFR-Targeted Therapy

Asel K. Biktasova[1], Duafalia F. Dudimah[2], Roman V. Uzhachenko[2], Kyungho Park[3], Anwari Akhter[4], Rajeswara R. Arasada[4], Jason V. Evans[4], Sergey V. Novitskiy[1], Elena E. Tchekneva[4], David P. Carbone[4], Anil Shanker[2,5], and Mikhail M. Dikov[4]

## Abstract

Activation of Notch signaling in hematopoietic cells by tumors contributes to immune escape. T-cell defects in tumors can be reversed by treating tumor-bearing mice with multivalent forms of the Notch receptor ligand DLL-1, but the immunologic correlates of this effect have not been elucidated. Here, we report mechanistic insights along with the efficacy of combinational treatments of multivalent DLL-1 with oncoprotein targeting drugs in preclinical mouse models of lung cancer. Systemic DLL-1 administration increased T-cell infiltration into tumors and elevated numbers of $CD44^+CD62L^+CD8^+$ memory T cells while decreasing the number of regulatory T cells and limiting tumor vascularization. This treatment was associated with upregulation of Notch and its ligands in tumor-infiltrating T cells enhanced expression of T-bet and phosphorylation of Stat1/2. Adoptive transfer of T cells from DLL1-treated tumor-bearing immunocompetent hosts into tumor-bearing SCID-NOD immunocompromised mice attenuated tumor growth and extended tumor-free survival in the recipients. When combined with the EGFR-targeted drug erlotinib, DLL-1 significantly improved progression-free survival by inducing robust tumor-specific T-cell immunity. In tissue culture, DLL1 induced proliferation of human peripheral T cells, but lacked proliferative or clonogenic effects on lung cancer cells. Our findings offer preclinical mechanistic support for the development of multivalent DLL1 to stimulate antitumor immunity. *Cancer Res; 75(22); 4728–41. ©2015 AACR.*



## Introduction

Notch is a family of evolutionarily conserved transmembrane receptors and ligands, and regulates a variety of processes in development and differentiation, including cell fate decisions (1). The mammalian Notch family includes four cell-bound Notch receptors, Notch1–4, and five Notch ligands DLL1, DLL3, DLL4, Jagged1, and Jagged2, which are also cell bound. Multiple downstream Notch target genes, including *Hes*, *Hey*, and *Deltex*, regulate the expression of various tissue-specific transcriptional activators (2, 3).

An important role for Notch has been proposed in the modulation of T-cell differentiation and immune responses. Evidence supports that Notch–DLL1 interaction can upregulate T-bet, stimulate IFNγ expression, and promote Th1 cell differentiation (4). Conditional transgenic expression of Notch1 intracellular domain (ICD) in antigen-specific $CD8^+$ T cells induced a central memory phenotype and increased cytotoxicity effects and granzyme B levels (5). Gain-of-function studies indicate that Delta-like Notch ligands (DLL) promote Th1 commitment of $CD4^+$ T cells (6, 7). By transactivating Th2-promoting target genes *IL4* and *Gata3*, Notch can also promote Th2 cell differentiation (8, 9). Although controversial, the bias is that Jagged ligands are associated with Th2-promoting Notch function (6, 10). Unlike other ligands, DLL3 is unable to activate Notch in cultured cells and seems to inhibit Notch signaling (11).

*In vivo*, overexpression or inhibition of Notch ligands on antigen-presenting cells (APC) suggested that APC-bound ligands might specify Th differentiation, with DLL and Jagged supporting Th1 and Th2 polarization, respectively (12–15). In addition to influencing Th1 and Th2 differentiation, an immunosuppressive function of Notch ligands has also been identified. Expression of Jagged ligands by APCs or hematopoietic progenitors favored generation of suppressive regulatory T cells (Treg) *in vivo* (16–18). Regulation of *IL17* and *RORγt* gene promoters and activation of Th17 differentiation has also been reported for Notch ligands (19). These data clearly confirm the immune modulatory function

[1]Department of Cancer Biology, Vanderbilt University Medical Center, Nashville, Tennessee. [2]Department of Biochemistry and Cancer Biology, Meharry Medical College School of Medicine, Nashville, Tennessee. [3]Department of Medicine, Vanderbilt University Medical Center, Nashville, Tennessee. [4]Division of Medical Oncology, Department of Internal Medicine, Ohio State University Medical Center, Columbus, Ohio. [5]Vanderbilt-Ingram Cancer Center, Nashville, Tennessee.

**Note:** Supplementary data for this article are available at Cancer Research Online (http://cancerres.aacrjournals.org/).

A.K. Biktasova, D.F. Dudimah, R.V. Uzhachenko, A. Shanker, and M.M. Dikov contributed equally to this article.

**Corresponding Authors:** Anil Shanker, Meharry Medical College School of Medicine, WBSB 2005, 1005 Drive DB Todd Jr. Boulevard, Nashville, TN 37208. Phone: 615-327-6460; Fax: 615-327-6442; E-mail: ashanker@mmc.edu; and Mikhail M. Dikov, Ohio State University Medical Center, 460 W. 12th Avenue, 484 BRT, Columbus, OH 43210. E-mail: Mikhail.Dikov@OSUMC.edu

**doi:** 10.1158/0008-5472.CAN-14-1154

of Notch ligands. However, no information is available on the role of Notch ligand-specific signaling in antitumor immune effector functions.

Our recent work revealed a mechanistic link in the molecular pathways underlying the tumor-induced perturbation of hematopoietic Notch signaling and demonstrated that altered expression of Notch ligands attenuated Notch signaling in the hematopoietic compartment of tumor-bearing host as a means of causing immunosuppression. This Notch-mediated immune suppression could be reversed by the enhanced DLL1-mediated Notch signaling in hematopoietic microenvironment (20–22). This predicted a novel therapeutic approach based on the stimulation of Notch signaling using soluble multivalent form of DLL1 to overcome cancer-associated immunosuppression, stimulate antitumor immunity and attenuate tumor growth.

In the present study, we evaluated the immunologic correlates of the systemic activation of Notch signaling using clustered DLL1 and its efficacy in combination with oncogene-targeted treatment in the mouse lung cancer model. We show that DLL1-based therapy can induce robust tumor antigen-specific T-cell effector and memory responses, enhance T-cell infiltration into the tumor, while decreasing Treg differentiation and tumor angiogenesis without increasing the tumorigenic potential of cancer cells. Such an activation of DLL1–Notch signaling suppressed tumor growth in wild-type mice as well as provided significant therapeutic benefit following an adoptive T-cell transfer into tumor-bearing SCID-NOD mice. Combined with mutant EGFR-targeted treatment by erlotinib, multivalent DLL1 significantly improved progression-free survival (PFS). This supports the potential therapeutic utility of multivalent Notch ligand in cancer treatment settings.

## Materials and Methods

### Cell lines

The human lung cancer cell lines (H157, H460, HCC15, HCC1437, HCC1264, and HCC2469) and murine Lewis lung carcinoma (LLC) cell line were obtained from the ATCC; low-passage (less than 10) cultures were used for the experiments. D459 cells are murine fibroblasts malignantly (murine fibrosarcoma) transformed in our laboratory by transfection of human *Ras* and mutant human *p53* (21, 23). Our laboratory is the primary source of these cells, and we regularly go back to reference stocks to ensure fidelity; routine sterility and *Mycoplasma* testing were performed regularly.

### Mice and tumor models

Female Balb/c, C57BL/6, and SCID/NOD mice (7- to 8-week-old) were purchased from The Jackson Laboratory. Mutant EGFR tetracycline-inducible transgenic mouse line that expresses an L858R mutant human EGFR in lung epithelial cells was described earlier and provided by Dr. William Pao (Vanderbilt University, Nashville, TN; ref. 24).

The animals were housed in pathogen-free units at the Vanderbilt University School of Medicine, in compliance with the Institutional Animal Care and Use Committee regulations. To induce tumor, mice were inoculated s.c. in flank with $0.3 \times 10^6$ D459 or LLC cells, as described previously (21, 25). For s.q. models, tumor volume was measured with calipers and tumor tissues were weighed at the endpoint of the experiments. In mutant EGFR mouse model, tumor growth was induced and sustained for the length of the experiment by providing mice with doxycycline in chow and the size of lung tumor was evaluated by MRI *in vivo*, as described previously (24). For this model, tumor recurrence was recorded when tumor volume exceeded by 30% the residual volume after erlotinib treatment.

### DLL1 clusters and treatment regimen

Mouse or human DLL1–Fc fusion protein is composed of the extracellular domain of mouse or human DLL1 and the Fc part of mouse IgG2A or human IgG1, respectively. To form DLL1 clusters, DLL1-Fc, biotinylated anti-IgG antibodies, and NeutrAvidin (Pierce) were mixed at a molar ratio of 1:4:10 in PBS, as described earlier (21, 26). As a control in all applications, Fc fragment of mouse IgG2 (Sigma-Aldrich) was used instead of DLL1–Fc. Mouse DLL1–Fc and biotinylated donkey anti-mouse IgG antibodies were from R&D Systems; human DLL1-Fc and biotinylated goat anti-human IgG antibodies—from Enzo Life Sciences, Inc.

Tumor-bearing mice received clustered DLL1 at doses of 0.15 μg/kg (4 μg/injection) of DLL1-Fc protein in 100 μL of PBS i.p. every other day (length of treatment is indicated in the figure legends and Results section). The control group received control clusters with Fc fragments instead of DLL1–Fc protein. Twice higher doses of clustered DLL1 were used in some experiments with similar results suggesting dose saturation of the clustered DLL1 effects.

In mutant EGFR tumor model, mice were treated with clustered DLL1 or control clusters, as above, from days 12 to 28 after tumor induction by doxycycline, whereas erlotinib was given during days 15 to 25 daily at a dose of 50 mg/kg, i.p., as previously described (24).

In separate experiments, nontumor mice Balb/c mice received clustered DLL1 or control clusters injections every other day for total of three times. Hematopoietic tissues from these mice were collected on the second day after the last injection and evaluated for the expression of Notch receptors, Notch ligands, and downstream Notch target genes *Hes1*, *Hey1*, and *Deltex* by qRT-PCR.

### Immunologic assays

D459 cells have a defined mutant p53 antigenic peptide (FYQLAKTCPVQL, aa 128-139; ref. 27). Induction of antigen-specific responses in this model was characterized by evaluation of IFNγ-producing T cells, as follows: splenocytes or LN cells from D459 tumor-bearing mice treated with clustered DLL1 or control clusters were stimulated with 10 μmol/L of mutant p53 or control peptide for 60 hours; IFNγ intracellular staining was performed using Mouse Intracellular Cytokine Staining Kit (BD Pharmingen) according to the manufacturer's recommendations. Data were acquired with FACSCalibur flow cytometer (BD Immunocytometry Systems). Gates were set on $CD8^+$ or $CD8^+CD44^+CD62L^+$ cells. LLC cells also have a defined antigenic peptide MUT1 (spontaneously mutated connexin 37, FEQNTAQP (28, 29). Splenocytes and lymph node (LN) cells ($2.5 \times 10^5$ cells/well) from LLC tumor-bearing mice treated with control or DLL1 clusters were stimulated with 10 μmol/L of MUT1 or control peptide for 48 hours and IFNγ-producing cells were enumerated by ELISPOT assay (CTL) according to the manufacturer's protocol. For the mutant EGFR model, lungs were assessed for the infiltration by IFNγ-producing cells and other immune cells. Lung single-cell suspensions were prepared, as described previously (25). IFNγ-producing cells were enumerated by intracellular staining and infiltration by immune lineages was assessed by flow

cytometry (see below). $CD45^+$ cells for evaluation of Notch signaling were isolated from lung single-cell suspensions, as described earlier (30).

Peptides were synthesized by the American Peptide Company, Inc.

### Flow cytometry

Fluorochrome-labeled cell-surface marker or intracellular protein specific antibodies were obtained from BD Bioscience Pharmingen and eBioscience, Inc. For staining of cell surface markers, cells were incubated with the antibodies for 20 minutes on ice. For intracellular cytokines, FoxP3, Stat, or phospho-Stat (p-Stat) cells were first stained for lineage-specific markers, and then permeabilized for 20 minutes with BD fixation/permeabilization kit and incubated with fluorochrome-labeled or unlabeled specific antibodies for 30 minutes on ice. When unlabeled primary antibodies were used, cells were washed, and then stained with fluorochrome-conjugated secondary antibodies. Matched fluorochrome-conjugated isotype IgG controls were used. Flow-cytometry data were acquired using a FACS LSR II (BD Immunocytometry) and analyzed with FlowJo software (Tree Star). Nonviable cells were excluded by using 7-amino actinomycin D. Antigen negativity was defined as having the same fluorescent intensity as the isotype control.

### Adoptive T-cell transfer

Splenocytes and tumor-draining LN cells from D459 tumor-bearing mice were collected on day 25 after inoculation of D459 cells and mixed; then, $5 \times 10^6$ cells were injected into retro-orbital plexus of SCID-NOD mice bearing palpable (3–4 mm) D459 tumors. Tumor growth was monitored and tumors weighted at the end of the experiment.

### Expression levels of Notch receptors, ligands and downstream targets, and transcription factors

Quantitative RT-PCR (qRT-PCR) was used to quantify expression of Notch downstream target genes, receptors and ligands as well as T-bet, Gata3, RORγt, and FoxP3 transcription factors in samples of mouse hematopoietic tissues or tumor cells using primers described earlier (21, 31). RNA was extracted with an RNeasy Mini Kit and possible genomic DNA contamination was removed by on-column DNase digestion using the RNase–free DNase set (Qiagen). cDNA was synthesized using the SuperScript III Reverse Transcriptase Kit (Invitrogen). cDNA, iQ SYBR green supermix (Bio-Rad) and gene-specific primers (see in Supplementary Table S1) were used in 20 μL PCR reactions as recommended by the manufacturer. Amplification of endogenous β-actin or GAPDH was used as internal controls.

### Western blot and ligand precipitation

Cells or tissues were lysed in a lysis buffer containing 20 mmol/L HEPES, 150 mmol/L NaCl, 10% glycerol, 1% Triton X-100, 1 mmol/L EGTA, and 1.5 mmol/L MgCl2 with set of inhibitors, as described previously (32). Equal amounts of protein were mixed with SDS sample buffer and separated by 7.5 or 10% SDS-PAGE, and transferred to polyvinylidene difluoride membrane (Amersham Biosciences). The following antibodies were used for detection: Notch1 (Cell Signaling Technology); Notch2 (Origene Technologies); Notch3 and DLL4 (Abcam); Notch4 (Millipore); Jag1 (Cell Signaling Technology); Jag2 (Thermo Scientific); DLL1 (Sigma-Aldrich); DLL4 (Abcam); GAPDH (Santa Cruz Biotechnology). All antibodies recognize epitopes in ICD of Notch.

To determine the interaction of clustered DLL1 with different Notch ligands, mouse thymus lysate in the above buffer was prepared and proteins were precipitated with a complex of DLL1-Fc with anti-Fc antibodies bound to protein-G magnetic beads (Pierce); as a control, Fc fragment was used instead of DLL1-Fc. Beads were then washed and mixed with SDS sample buffer for the subsequent Western blot analysis of bound proteins.

Note that as full-length Notch is composed of two noncovalently bound domains, on Western blot analysis in denaturing/reducing conditions with antibodies to ICD epitopes, it appears as ICD band of approximately 110 kD or 90 kD for Notch1 and 2 or Notch3 and 4, respectively. In some cases, in cancer cells where Notch expression is high, full-length Notch could also be seen under these conditions.

### Immunohistochemistry

Tumor tissue was extracted, fixed in 10% formalin, embedded in paraffin, and sectioned (5 μm). Slides were stained with peroxidase-labeled antibodies to the CD3e (Santa Cruz Biotechnology), CD11b, Gr1, or CD34 cell surface markers (Novus Biologicals). The number of cells or tumor blood vessels identified by peroxidase substrate staining was counted using a Nikon Eclipse E600 with a 40×/1.0 NA Plan Apochromat oil objective (Nikon Instruments) and with Olympus DP-11 digital camera (Olympus America). Images were processed using Meta-Morph 5.0.7 (Universal Imaging) and ImageJ (NIH, Bethesda, MD) software.

### Cell proliferation and colony-forming assays

Human peripheral blood was drawn from healthy consented donors according to the protocol approved by the Vanderbilt University School of Medicine Internal Review Board. Peripheral blood mononuclear cells (PBMC) were isolated by gradient centrifugation using Ficoll-Paque (GE Healthcare). Proliferation of T cells was measured using the intracellular dye carboxyfluorescein succinimidyl ester (CFSE; Molecular Probes; Life Technologies). PBMC were stimulated with Dynabeads Human T-Activator (anti-CD3, anti-CD28, and anti-CD137 antibodies coupled to beads; Life Technologies), as recommended by the manufacture, with 0.5 μg/mL multivalent DLL1 (based on DLL1-Fc protein) or control clusters for 4 days. T-cell proliferation was assessed by CFSE dilution in $CD3^+$ cells by flow cytometry.

To evaluate the proliferation of human and murine cancer cells, cells were seeded in 96-well plates and cultured for 16 hours in DMEM medium supplemented with 10% FBS. Then, 1 μg/mL clustered DLL1 (based on DLL1-Fc protein) or control clusters were added and cells were cultured for additional for 24 hours; for the last 2 hrs of incubation 1 μCi [3H-thymidine] per well was added and [3H-thymidine] incorporation was assessed by liquid scintillation counting, as described earlier (33).

Colony formation of human lung cancer cells in soft agar was performed, as previously described (34), with 2,500 cells seeded in 6-well plate in DMEM with 10% FBS. Colonies were counted after 2 weeks.

### Statistical analysis

Data were analyzed using the GraphPad Prism 4.0 software (GraphPad Software Inc.) and presented as mean ± SEM. Comparisons between treatment and control groups were performed

using one-way ANOVA followed by Dunnett's posttests. Comparisons between two groups were performed using two-tailed unpaired *t* tests. Survival curves were compared using the Mantel–Haenszel log rank test. Values were considered statistically significant when a *P* value was less than 0.05.

## Results

### Multivalent DLL1 interacts with Notch receptors and upregulates hematopoietic Notch signaling *in vivo*

Activation of Notch receptor proteolytic cleavage and signaling requires a multivalent interaction between Notch receptors and ligands, whereas soluble forms of ligands act as Notch inhibitors (35). In this study, we used a multivalent or clustered form of DLL1, which was a complex of DLL1–IgG Fc fusion proteins with biotinylated anti-Fc antibody and avidin (21), acting as an activator of Notch.

Notch system appears to be very sensitive to modulation by its ligands. We performed ligand precipitation experiments to determine the Notch receptors that bind clustered DLL1. DLL1-Fc–anti-Fc antibody complex or Fc–anti-Fc antibody complex, as a control, were bound to protein G magnetic beads and the beads were added to the mouse thymus lysate to pull down the interacting Notch receptors. Western blot analysis of the precipitated proteins revealed that all four Notch receptors interact with clustered DLL1, thus suggesting that each of them could be involved in mediation of the observed effects of the enhanced DLL1 signal (Fig. 1A).

To explore the effects of clustered DLL1 on hematopoietic Notch system *in vivo*, clustered DLL1 was injected in healthy mice i.p. every other day for a total of three doses and Notch signaling was evaluated on the second day after the last administration. qRT-PCR analysis demonstrated that such treatment sustained significantly elevated levels of Notch target genes (Fig. 1B). The clustered DLL1 reagent seems to deliver activating DLL1 signals to all hematopoietic organs, as changes in the expression of one or more Notch genes are detectable in all organs except LNs, which could be due to the low vascularization/circulation of LNs or be an attribute of the Notch system response in LN cells.

Clustered DLL1 also altered receptor and ligand expression patterns in these sites (Fig. 1C and D). The expression pattern of Notch receptors and ligands appears to be tissue specific. Bone marrow, blood, and spleen show significantly increased Notch signaling as well as the expression of Notch ligands following clustered DLL1 administration (Fig. 1C and D). High levels of Notch ligand expression in these organs might associate with the high number of myeloid cells, which are known to be a source of Notch ligands for the differentiating lymphocytes (6, 7). The magnitude of Notch receptor expression changes is highest in the spleen and thymus, which corresponds to the high number of lymphoid cells in these tissues—the recipients of the activating signals from the ligands (Fig. 1C). The increased expression of Notch receptors and ligands upon pharmacologic DLL1-mediated stimulation may result in the amplification of the initial signal. This might explain why relatively low doses of clustered DLL1 produce significant biologic effects.

### Pharmacologic enhancement of DLL1-mediated Notch signaling supports effector T-cell differentiation and survival in tumor-bearing mice

Notch signaling plays an important role in regulating differentiation of naive $CD4^+$ T cells into distinct Th lineages. We found that systemic administration of clustered DLL1 in LLC tumor-bearing mice stimulated phosphorylation of Stat1 and Stat2 transcription factors in $CD4^+$ T cells (Fig. 2A and B) that are associated with Th1 differentiation. Enhanced Stat1 signaling in $CD4^+$ T cells from DLL1-treated mice correlated with the increase in the expression of *T-bet*—a mediator of transcriptional effects of Stat1 on T-cell differentiation. Among the lineage-specific transcription factors involved in the regulation of Th cell differentiation, only *T-bet* gene expression displayed significant upregulation, whereas expression of *Gata3*, *RORγt*, and *FoxP3* genes, as analyzed in a pool of splenocytes and LN cells from treated LLC-bearing mice, did not show any significant change (Fig. 2C). Statistically significant upregulation in phosphorylation of Stat3, responsible for the survival of activated T cells (22), was also detected, thus suggesting improved T-cell survival (Fig. 2A).

### Clustered DLL1 therapy improves antitumor T-cell function and memory

We demonstrated earlier using different mouse models that therapeutic enhancement of DLL1/Notch signaling produces significant T-cell–mediated attenuation of tumor growth (21). Here, we investigated whether such therapy is capable of enhancing tumor-specific immune responses and generating specific tumor-protective T-cell memory in lung tumor models, LLC and D459, where tumor-specific antigenic peptides have been identified, thus allowing the assessment of tumor-specific immune responses.

Treatment of mice with clustered DLL1 or control cluster for 10 days after s.c. injection of LLC cells elicited strong antigen-specific CTL response to the endogenous LLC tumor antigen MUT1. Higher number of IFNγ-secreting cells were noted in spleens and LNs of mice treated with DLL1 clusters than in the control group after restimulation with tumor antigenic peptide MUT1 (Fig. 2D). This correlated with significantly smaller tumor mass in clustered DLL1-treated mice than in control clusters-treated animals (not shown). These results suggest high efficacy of clustered DLL1 as an immunization adjuvant.

In D459 model, s.c. tumor appeared on days 7 to 8 after cell inoculation and developed rather slowly for an additional 10 to 12 days, after which tumor grows exponentially (Fig. 3A). Clustered DLL1 or control clusters were administered after tumors were established (tumor diameter 4–5 mm) from days 7 to 19 every other day (Fig. 3A). Clustered DLL1 delayed tumor growth when compared with the control cluster (Fig. 3A). Immunologic parameters were examined on day 21 when the differences in tumor size in control and clustered DLL1 groups were still insignificant. This excluded variations in the systemic immunologic effect due to tumors of differing sizes. Significantly higher levels of T-cell activation marker CD25 and intracellular IFNγ production were observed in the splenic and LN $CD8^+$ T cells following re-challenge with D459 tumor antigenic–mutant p53 peptide (Fig. 3B). Moreover, multivalent DLL1 therapy resulted in a significant increase of splenic $CD44^+CD62L^+$ $CD8^+$ T cells characterized as central memory effector T cells (Fig. 3C and D). Among $CD44^+CD62L^+$ $CD8^+$T cells, there were significantly more IFNγ-producing T cells after re-stimulation with the cognate-mutant p53 peptide, thus indicating increased number and function of tumor-specific memory T cells (Fig. 3E). In addition to stimulating robust antigen-specific T-cell responses, systemic activation of DLL1/Notch signaling resulted in moderate, but statistically significant reduction of the number of regulatory T cells in

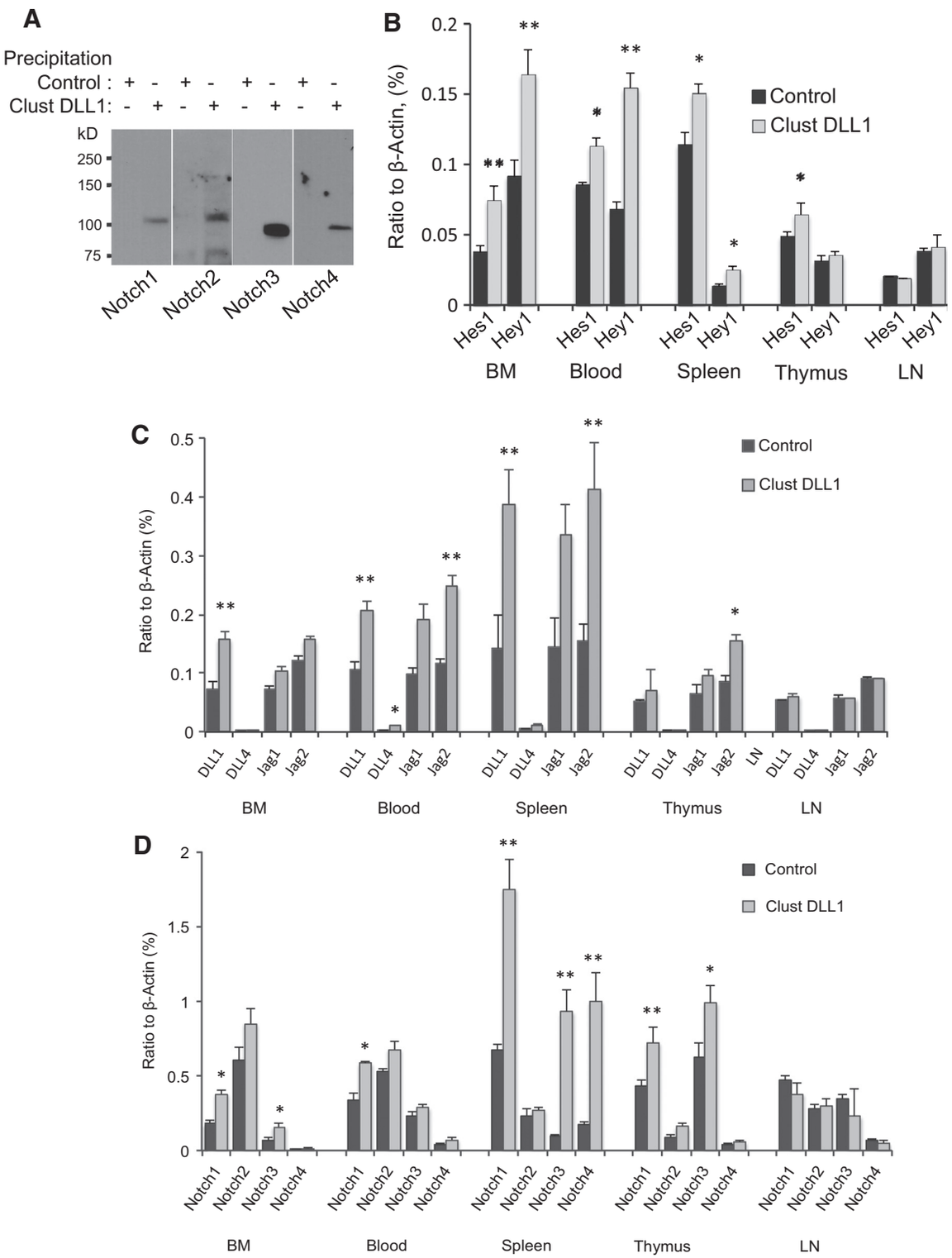


**Figure 1.**
Clustered DLL1 binds to four Notch receptors, upregulates Notch signaling, and modulates expression of hematopoietic Notch genes *in vivo.* A, precipitation of Notch receptors from mouse thymus lysate by DLL1-Fc/anti-Fc antibody or Fc/anti-Fc antibody (control) complexes bound to protein G beads; precipitated proteins were separated by Western blot analysis and visualized using antibodies to Notch 1, 2, 3, or 4. B–D, mRNA expression of downstream Notch target genes *Hes1* and *Hey1* (B), Notch ligands (C), and Notch receptors (D) in hematopoietic organs of mice treated with clustered (clust) DLL1. Mice received three injections of clustered DLL1 or control clusters i.p. every 2 days. Gene expression was evaluated on the second day after the last injection by qRT-PCR. Mean ± SEM, 6–8 mice per group, *, $P < 0.05$; **, $P < 0.01$. BM, bone marrow.

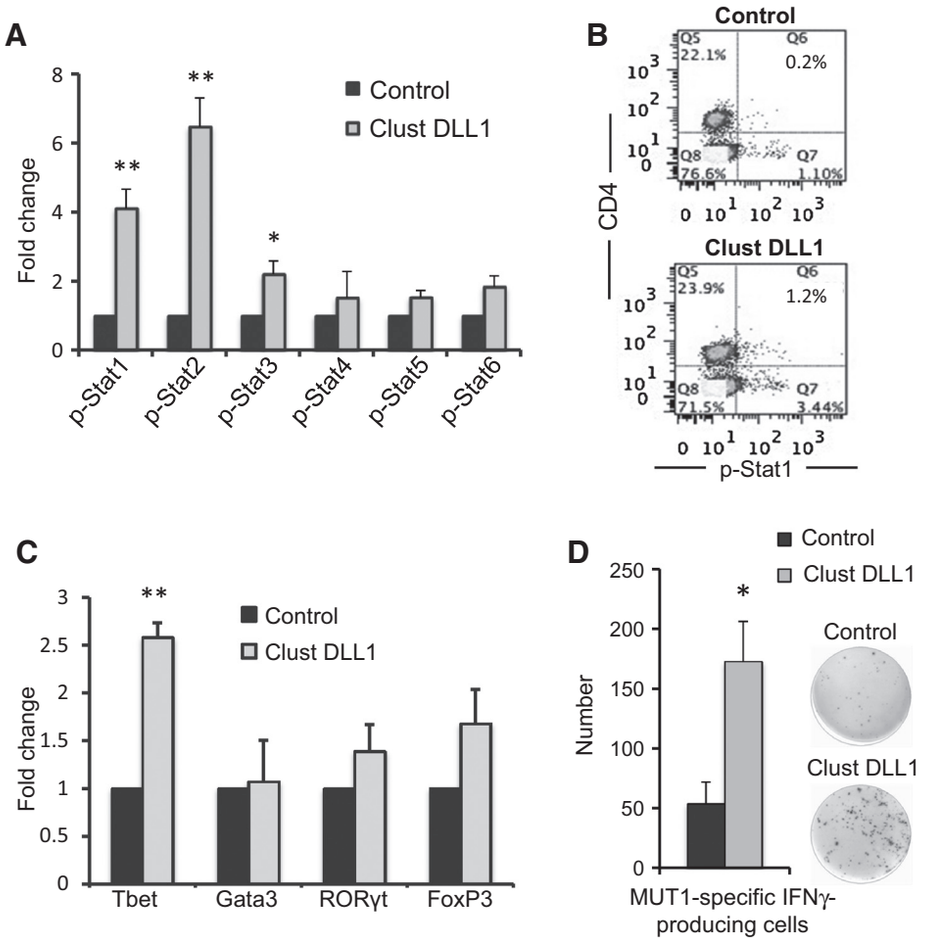


**Figure 2.**
Enhancement of DLL1-mediated Notch signaling promotes T-cell differentiation and survival in tumor-bearing host and elicits tumor antigen–specific CTL responses in tumor-bearing mice. LLC tumor-bearing mice were treated with clustered DLL1 or control clusters i.p. every 2 days for 10 days. Gene expression or Stat phosphorylation was evaluated by qRT-PCR or intracellular protein immunofluorescence staining, respectively, in a pool of splenocytes and LN cells; expressed as fold increase in clustered DLL1-treated mice over the control clusters group. A, changes in phospho-Stat proteins in gated $CD4^+$ cells following intracellular flow-cytometry staining. B, representative phospho-Stat1 versus CD4 dot plot. C, expression of transcription factors regulating T-cell differentiation assessed by qRT-PCR. Mean ± SEM; 5 mice per group; *, $P < 0.05$; **, $P < 0.01$. D, IFNγ-producing cells to endogenous LLC tumor antigen MUT1 were enumerated by ELISPOT assay in a mixture of splenocytes and LN cells of LLC tumor-bearing mice treated with control or DLL1 clusters following restimulation *in vitro* with tumor antigenic peptide MUT1 for 48 hours. Mice received clustered DLL1 or control treatment for 10 days immediately after injection of LLC cells. Mean ± SEM; 5 mice per group; *, $P < 0.05$.

the spleen of treated animals (Fig. 3F). The combination of these effects might have contributed to the observed inhibitory effect on tumor growth.

Induction of DLL1-induced T-cell effector memory and protective immunity was further confirmed in the adoptive T-cell transfer experiments. A total lymphocyte fraction from a pool of splenocytes and tumor-draining LN cells, to have a higher frequency of tumor antigen-specific T cells, from D459 tumor-bearing Balb/c mice treated with clustered DLL1 or control clusters were transferred i.v. into SCID-NOD mice bearing palpable D459 tumors. Lymphocytes transferred from clustered DLL1-treated donors, but not from the control-treated animals, significantly attenuated tumor growth in SCID-NOD mice (Fig. 4A and B).

These data strongly suggest that the multivalent DLL1-mediated Notch activation possesses functional capacity to induce tumor-specific T-cell responses and memory, resulting in the significant therapeutic benefit in tumor models. They imply strong association of the DLL1–Notch axis in regulation of the T-cell–mediated antitumor immunity.

### Increased tumor infiltration by immune cells and decreased tumor vascularization in mice treated with clustered DLL1

Additional effects of the pharmacologic DLL1-mediated Notch activation in tumor-bearing host associate with remarkably higher (2.65-fold) T-cell infiltration into tumors as assessed by CD3e immunostaining of D459 tumor sections (Fig. 4C), a factor known to correlate with the improved prognosis in human patients (36). In this model, no significant differences were found in the number of tumor-infiltrating $Gr1^+$ or $CD11b^+$ myeloid cells between clustered DLL1-treated and control groups (data not shown). D459 tumors staining with endothelial marker CD34 revealed significantly decreased vascularization of tumors in multivalent DLL1-treated animals than in control animals (Fig. 4D). This result is in line with the observation that DLL1-induced Notch signaling has suppressive effect on tumor growth in B16 melanoma model due to the attenuated vascularization (37).

These data suggest that the antiangiogenic effect of multivalent DLL1 therapy together with the enhanced antitumor T-cell responses contribute to tumor-inhibitory effects in therapeutic settings.

### Clinical and immunologic effectiveness of the multivalent DLL1 in combination with mutant EGFR oncogene–targeted therapy associates with the enhanced Notch signaling and improved immune responses

We tested multivalent DLL1 therapy in combination with mutant EGFR oncogene–targeted inhibition in the EGFRL858R transgenic mouse model. Treatment of patients with tumors

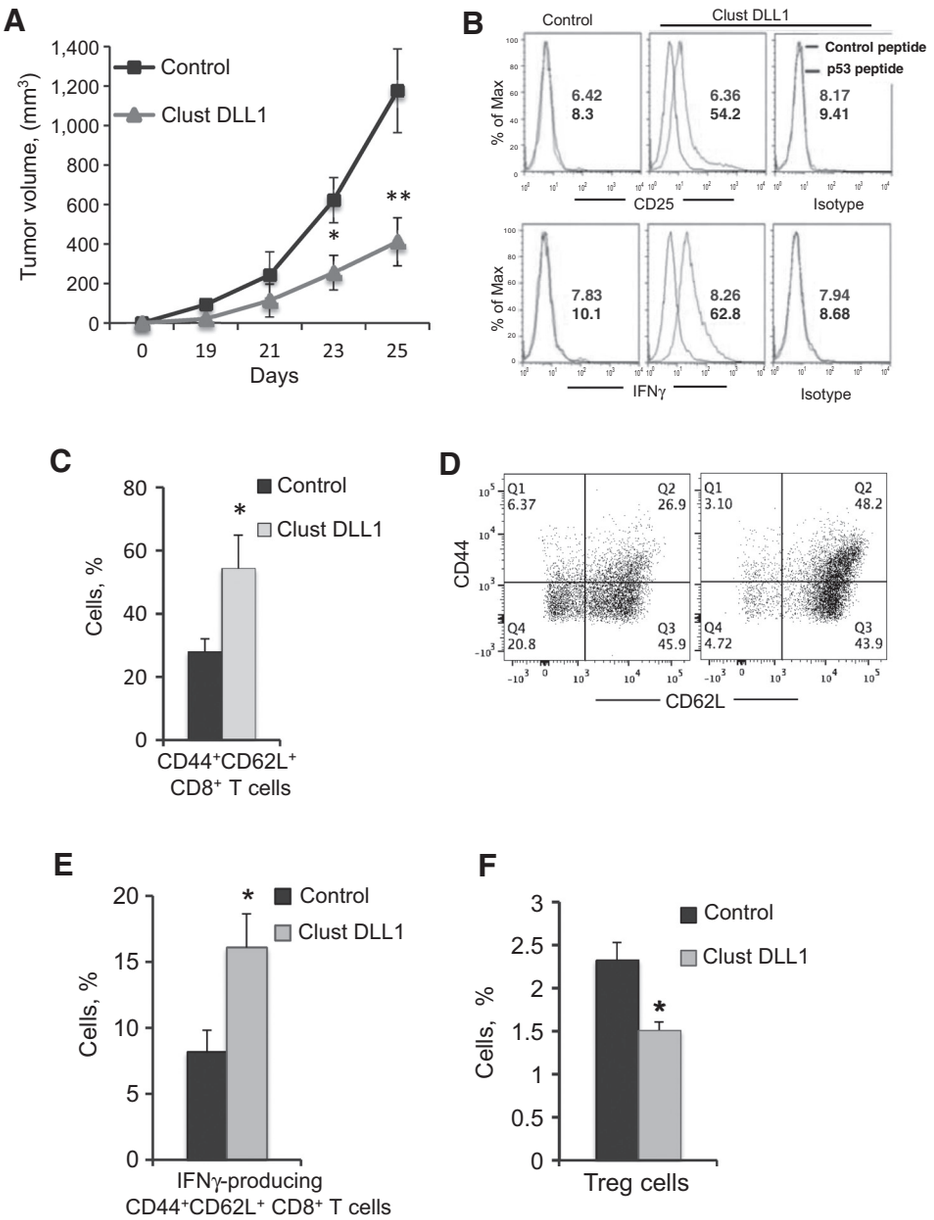


**Figure 3.**
Attenuation of tumor growth by clustered DLL1 correlates with the improved antitumor T-cell immunity. Mice inoculated with D459 tumor cells were treated with clustered DLL1 or control clusters i.p. every 2 days from days 7 (after tumors reached 4–5 mm) to 19. A, D459 tumor growth. Mean ± SEM; 8 mice per group; *, $P < 0.05$; **, $P < 0.01$. B, surface expression of activation marker CD25 and intracellular staining for IFNγ in cultures of splenic $CD8^+$ T cells isolated from mice on day 21 following restimulation *in vitro* with p53 D459 tumor antigenic or control peptide for 60 hours. Numbers—mean fluorescence intensity for control (left) and cognate (right ) peptide-stimulated cells. Representative histograms of total 4. C, proportion of memory $CD44^+CD62L^+CD8^+$ T cells in splenocytes of mice. D, representative CD44 versus CD62L flow cytometry dot plot on gated splenic $CD8^+$ T cells from a total of 5 mice. E, increased number of IFNγ-producing T cells within splenic $CD44^+CD62L^+$ memory $CD8^+$ T-cell population. F, decreased number of regulatory T cells in spleen of clustered DLL1 compared with control cluster-treated animals. C, E, F, mean ± SEM; 5 mice per group; *, $P < 0.05$.

bearing activating EGFR mutations with EGFR inhibitors represents an example of successful oncogenic pathway–targeted therapy. EGFR gene in-frame deletions in exon 19 and L858R mutation in exon 21 constitute nearly 90% of the lung adenocarcinoma somatic-activating mutations and have been associated with sensitivity and rapid clinical response to the EGFR tyrosine kinase inhibitors (TKI) gefitinib and erlotinib (38, 39). However, in most of responding patients, the cancer resumes detectable growth within several months (38, 40). We tested whether integrating the multivalent DLL1-based immunotherapy with oncogene-targeted TKI would induce sustained immune responses and long-lasting remission in sensitive tumors. We used a tetracycline-inducible transgenic mouse line that expresses an L858R-mutant human EGFR in lung epithelial cells (24). The expression of *EGFR* mutant leads to the development of lung adenocarcinomas in 2 to 3 weeks after doxycycline induction with erlotinib treatment causing rapid tumor regression (24). In our regimen, during the doxycycline tumor induction, mice received two injections of clustered DLL1, and then a combination of erlotinib with clustered DLL1 followed by two more injections of clustered DLL1; mice then were left untreated (Fig. 5A). The control group received control clusters instead of multivalent DLL1. Tumor size was monitored at different time points by MRI with tumor recurrence determined when the volume of tumor exceeded the residual tumor volume after erlotinib treatment by 30%. EGFRL858R mutant mice were highly responsive to the clustered DLL1 combination therapy, as seen by the decreased lung tumor burden and significantly improved PFS (Fig. 5A and B).

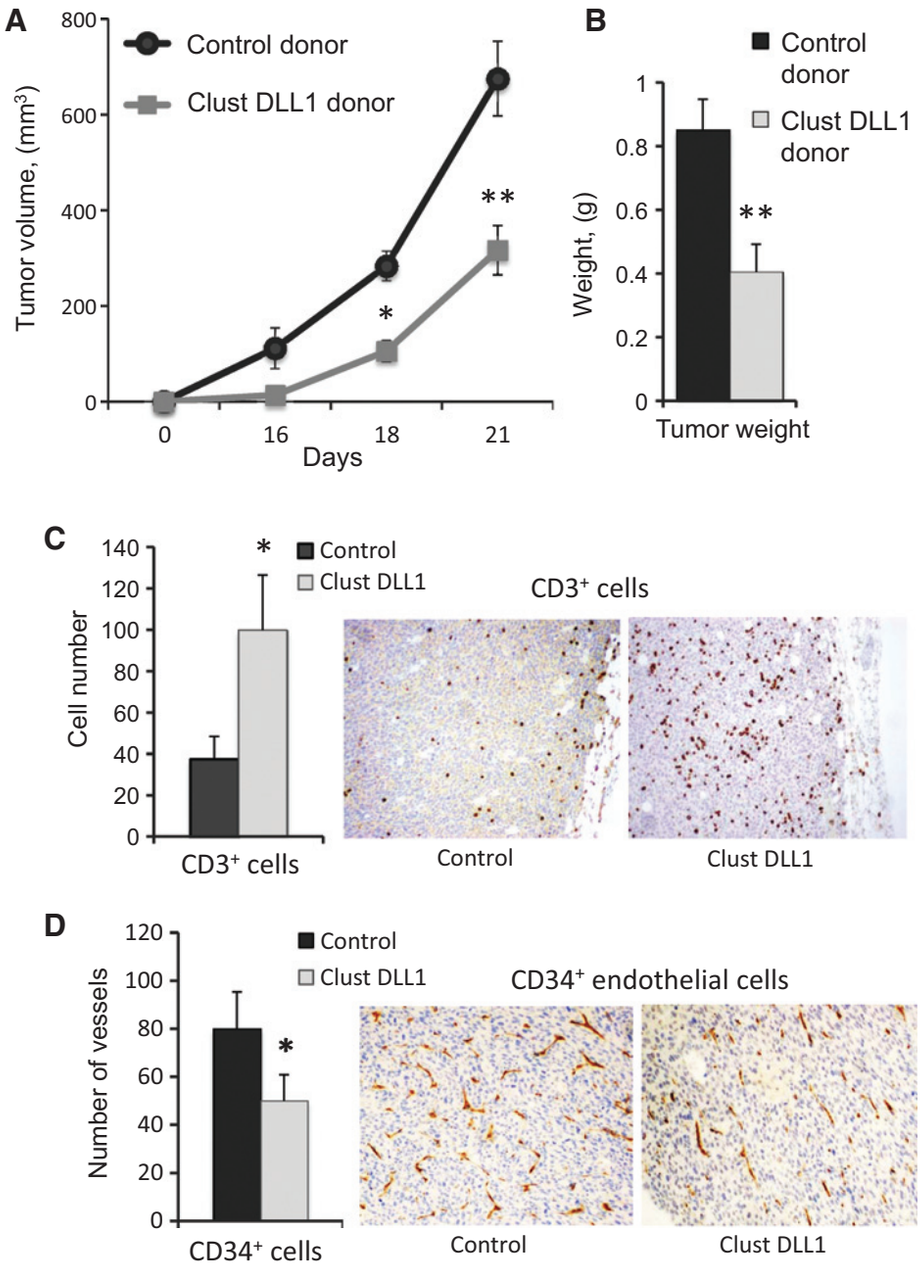


**Figure 4.**
Multivalent DLL1 therapy elicits tumor antigen-specific T-cell memory, enhances tumor infiltration by T cells, and attenuates tumor angiogenesis. D459 tumor growth (A) and weight (B) in SCID-NOD mice that received lymphocyte transfer from donor mice bearing D459 tumor and treated with clustered DLL1 or control clusters. A total of $5 \times 10^6$ cells of the total lymphocyte fraction from a pool of RBC-depleted splenocytes and tumor-draining LN cells were harvested from donor mice at day 21 (see Fig. 3) and transferred into SCID-NOD mice bearing palpable (3–4 mm) D459 tumors at day 5. Mean ± SEM; 5 SCID-NOD mice per group; *, $P < 0.05$; **, $P < 0.01$. C and D, immunostaining of tumor tissues with CD3ε (C) or CD34 (D) antibodies. D459 tumor-bearing mice were treated with DLL1 or control clusters, as in Fig. 3, and tissue sections were prepared on day 21. Representative images and the numbers of infiltrating $CD3\varepsilon^+$ T cells or $CD34^+$ tumor vessels are presented. Mean ± SEM; 5 mice per group; 10 fields on two nonadjacent sections were counted for each sample; *, $P < 0.05$.

Analysis of the hematopoietic Notch signaling, protein expression, and immunologic parameters revealed that the observed therapeutic effects correlated with the enhanced Notch signaling and improved immune responses (Fig. 6). Treatment with multivalent DLL1 significantly upregulated the expression of downstream Notch targets *Hes1*, *Hey1*, and *Deltex1* in lung-infiltrating immune cells of tumor-bearing EGFRL858R transgenic animals as well as enhanced the expression of splenic Delta-like ligands, Jag2 and Notch1, 2, and 3 receptors, thus apparently reversing previously observed tumor-induced deficiency in hematopoietic Notch signaling and ligand expression (Fig. 6A and B; ref. 21). Administration of clustered DLL1 resulted in significant alterations in the numbers of immune cells infiltrating the diseased lungs. We found remarkably increased numbers of INFγ-producing T cells and $CD11b^+CD11c^{high}$ dendritic cells (DC), despite the moderate decrease in the total infiltrating $CD3^+$ T cells. Worth noting is also the increased number of $CD19^+$ B cells (Fig. 6C). The data suggest that the enhancement of DLL1/Notch signaling provides benefit in combination treatment with oncogene-targeted drugs due to the improved antitumor immunity.

### DLL1-Notch signaling enhances human peripheral T-cell proliferation without directly stimulating tumorigenicity

In human adults, peripheral T cells play a key role in mediating immune responses. We thus tested whether multivalent DLL1 would have direct effect on human peripheral

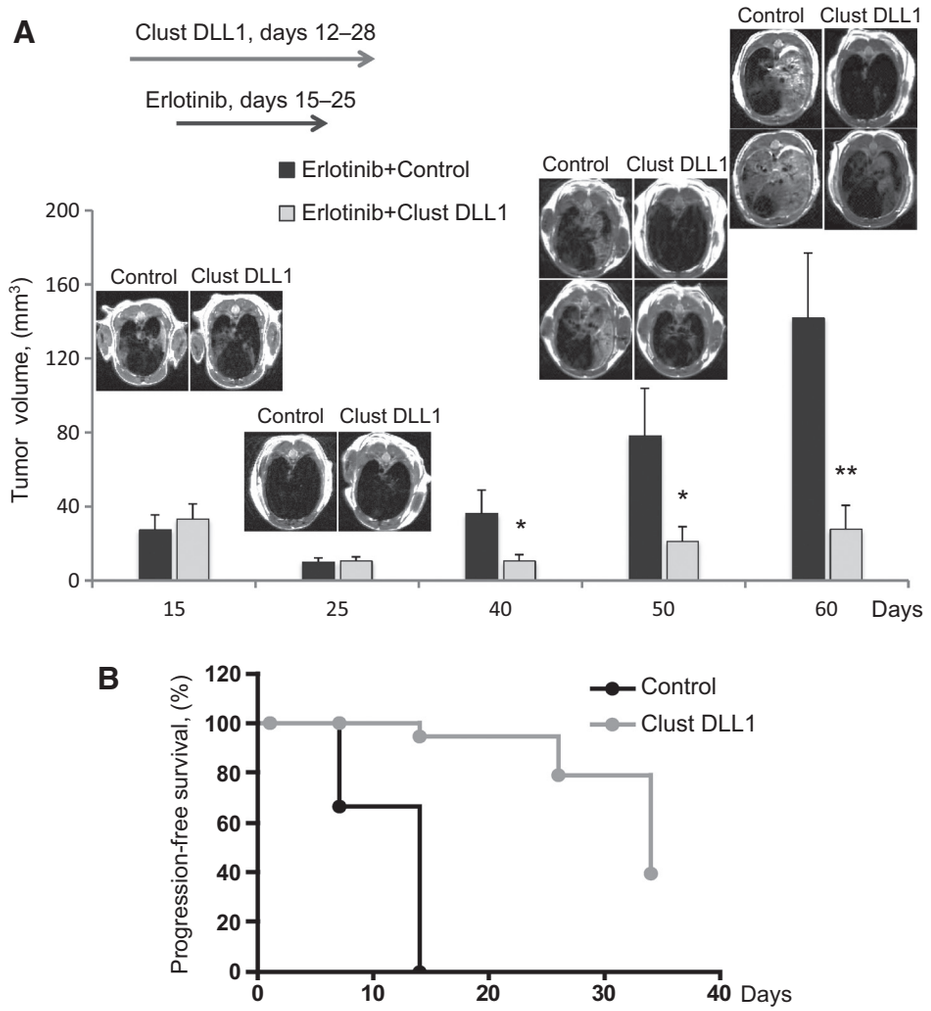


**Figure 5.**
Multivalent DLL1 significantly improves PFS in combination with EGFR oncogene–targeted treatment in the EGFRL858R transgenic mouse model. Transgenic *EGFRL858R* mice with induced lung tumors were treated with erlotinib in combination with clustered DLL1 or control clusters, as shown in A. A, lung tumor (white opacities) growth was evaluated by MRI and volume quantified. Insets, representative MRI images at the corresponding time points. B, PFS; recurrence was determined when tumor volume exceeded by 30% residual tumor volume after erlotinib treatment. Mean ± SEM; 8 mice per group; *, $P < 0.05$; **, $P < 0.05$.

T-cell function. PBMCs from human donors were stimulated with beads-coupled CD3, CD28, and CD137 antibodies with or without multivalent DLL1 for 4 days. Proliferation of gated $CD3^+$ T cells, as assessed by CFSE dilution, demonstrated that clustered DLL1 enhanced proliferation of human peripheral T cells (Fig. 7A).

The pleiotropic functions of Notch and complex effect of interference with this signaling pathway raise legitimate safety concerns regarding systemic activation of Notch signaling by the multivalent DLL1. We assessed the effect of this reagent on tumorigenic properties of different human lung and mouse cancer cells. Various tumor cell lines that we tested expressed Notch receptors (Fig. 7B) and showed varying kinetics and levels of RNA expression of target genes, *Hes1* and *Hey1* following culture with mouse or human multivalent DLL1 (Supplementary Fig. S1). However, of high clinical significance is the fact that this activated signaling did not translate into the increased proliferation or clonogenicity of tumor cells (Fig. 7C and D). Rather, clustered DLL1 had antiproliferative and/or anticlonogenic effect on some tumor cells (H157, H460, HCC2429 and H460, H1437, respectively; Fig. 7C and D). Moreover, DLL1-treated mice showed no clinically abnormal behavior or any difference in body or organ weight compared with the control mice. No gross abnormalities were noted, nor was there any substantial changes in the numbers of red or white blood cells, lymphocytes or platelets counts in the peripheral blood following DLL1 treatments (data not shown).

## Discussion

T-cell immune surveillance against tumors is well established. However, induction of tumor-induced deficiencies in T-cell differentiation and function is a fundamental mechanism for tumor escape from the host immune system. We reported earlier a previously unidentified mechanism for tumor-associated defects in T lymphocytes mediated by the alteration of the expression pattern of Notch ligands and reduced Notch signaling in the hematopoietic compartment. Selective systemic activation of Notch signaling by a multivalent form of DLL1 resulted in significant attenuation of tumor growth in a T-cell–dependent manner in tumor models (21). The current study elucidates the immunologic consequences of the pharmacologic enhancement of DLL1 signaling and tests the hypothesis that the multivalent DLL1-based immunotherapy would benefit the oncogene-targeted treatments.

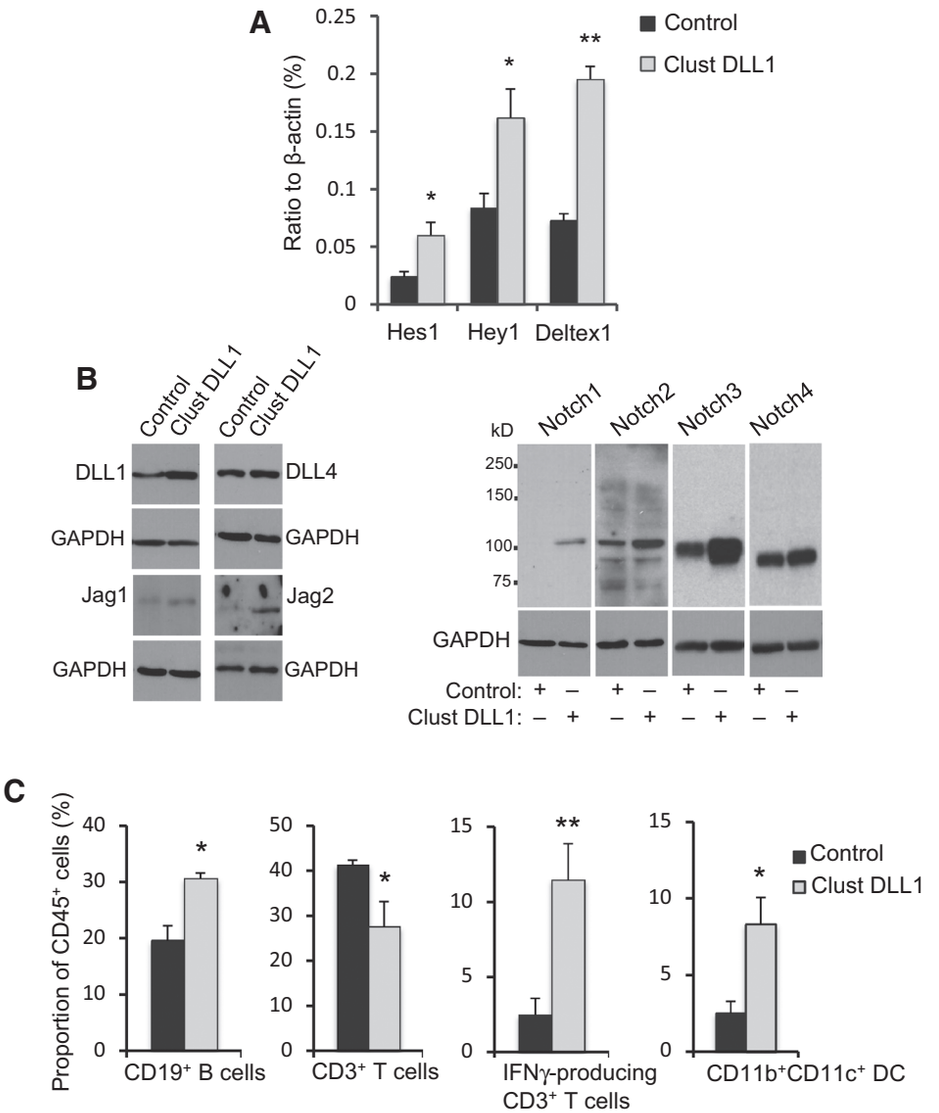


**Figure 6.**
Clustered DLL1 enhances Notch signaling, modulates expression of Notch genes in hematopoietic compartment, and provides immunologic benefit in combination with EGFR inhibition in the *EGFRL858R* transgenic lung cancer mouse model. Lung tumors were induced and mice treated with erlotinib in combination with clustered DLL1 or control clusters, as in Fig. 5. For immunologic assays and analysis of lung-infiltrating immune cells, single-cell suspensions from lungs were prepared on day 50 after tumor induction. A, mRNA expression of downstream Notch target genes in $CD45^+$ cells isolated from mouse lungs. B, protein expression of Notch ligands and receptors in splenocytes. C, proportion of lung infiltrating immune cell lineages. Mean ± SEM, $n = 5$; *, $P < 0.05$; **, $P < 0.01$.

Notch system appears to be highly responsive to the modulation by its ligand. The effects included not only increased downstream signaling but also a selective upregulation of Notch family receptor and ligand expression in the hematopoietic organs. These results suggest the potential existence of an autocrine amplification loop in the Notch system, where the initial receptor–ligand signal is further amplified via upregulation of the Notch system components. It would be clinically important to consider such autocrine amplification of Notch signaling from a potential therapeutic intervention point, as studies indicate that the effect of Notch modulation might be dose-dependent (41, 42). Our experiments revealed that clustered DLL1 binds to all four Notch receptors. Additional investigations would be required to identify the role of each of the receptors as well as their potential heterodimeric interaction with the multivalent ligand in mediating the observed effects and to determine whether they are DLL1-specific and how other ligands modulate Notch gene expression.

Stimulation of Notch signaling with multivalent DLL1 has significant positive effect on T-cell–mediated antitumor immunity. It induces tumor antigen-specific IFNγ production by $CD8^+$ T lymphocytes, increases the pool of central-memory $CD8^+$ T cells and enhances IFNγ synthesis within central memory $CD8^+$ T-cell population. These results imply the capacity of DLL1 to induce effector T cells *in vivo*. Differentiation of T cells into effector and memory subsets is dependent on the status of Stat activation, including their phosphorylation. Activation of Stat1, Stat2, Stat4, and Stat6 promotes Th1-type response, activation of Stat5 signaling pathway drives Th2 differentiation whereas Stat3 supports Th17 stemming in activated T cells via inhibition of T-bet and stimulation of RORγt transcription factor (30). The DLL1–Notch axis appears to be actively involved in the regulation of Stat signaling by enhancing phosphorylation of Stat1 and Stat2. This supports Th1 profile of T cells together with the upregulation of T-bet involved in the transcriptional effects of Stat1 on T-cell differentiation and IFNγ

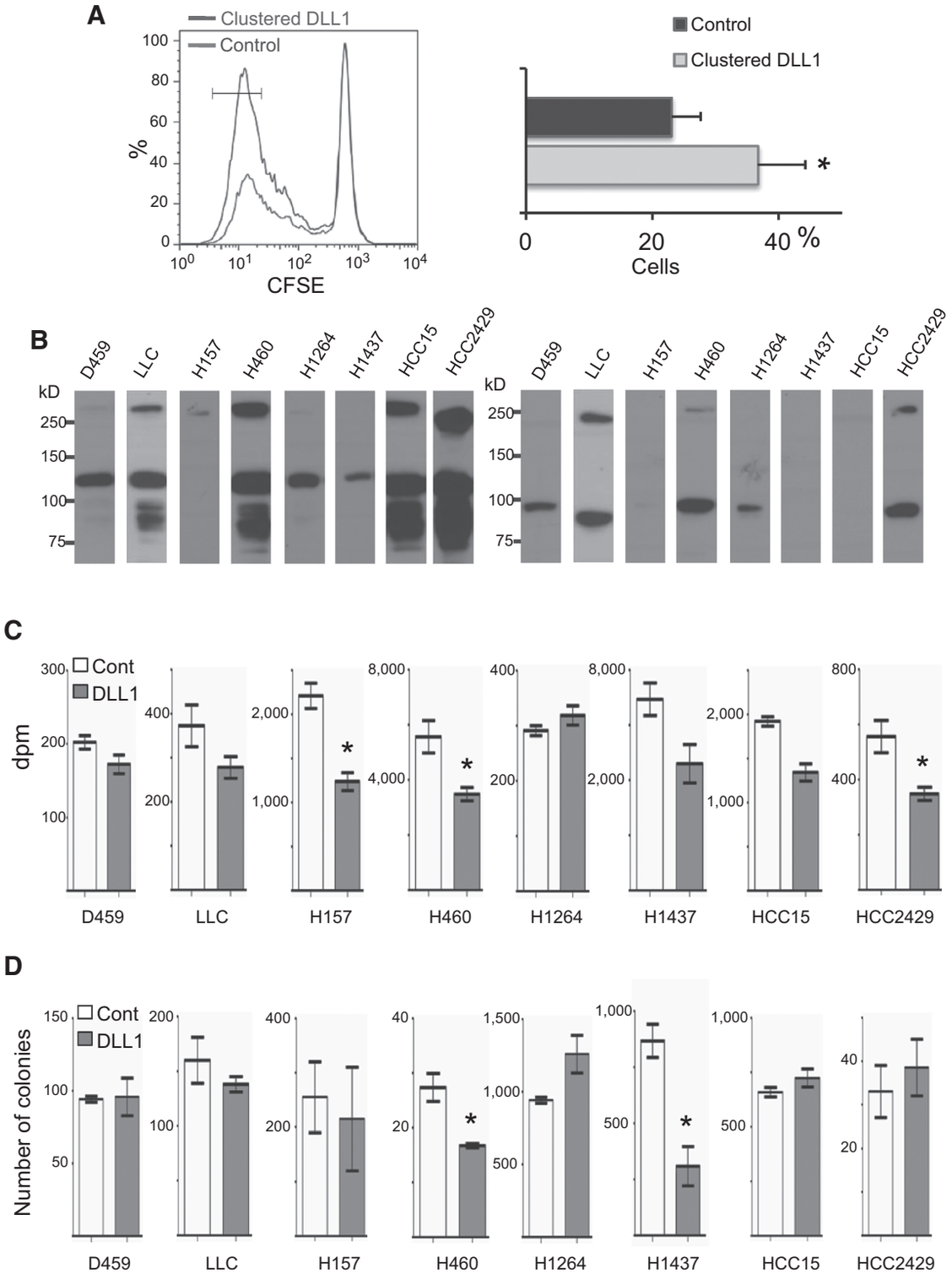


**Figure 7.**
DLL1-induced Notch signaling enhances human peripheral T-cell proliferation without any protumorigenic effects on cancer cells *in vitro*. A, PBMCs from human donors were stimulated with beads-coupled CD3, CD28, and CD137 antibodies with or without multivalent DLL1 for 4 days. Gated $CD3^+$ T-cell proliferation was assessed by CFSE dilution. Representative histogram overlays (higher peak, clustered DLL1) as well as day 4 total cell yields are shown. Mean ± SEM; $n = 4$; $^*P < 0.05$. B, expression of Notch1 and Notch3 in mouse and human cancer cell lines assessed by Western blotting. Notch1 (left) and Notch3 (right) bands at approximately 110 kD and 90 kD, respectively, correspond to ICD; higher bands at approximately 250 kD represent full-length Notch (see also note for Western blot analysis in Materials and Methods). C, cell proliferation measured by [3H]-thymidine incorporation. D, colony formation in soft agar evaluated after 2 weeks. Mean ± SEM; $n = 4$. Both PBMC and cancer cells were cultured with clustered DLL1 or control clusters at 1 μg/mL of DLL1-Fc protein.

production, but not the other transcription factors regulating Th cell differentiation (31). Stat1 sustains $CD8^+$ T-cell memory pool by increasing cell survival after their antigen-specific activation (32). This explains the higher rate of $CD8^+$ central-memory T cells after clustered DLL1 treatment. Although clustered DLL1 also elevated Stat3 phosphorylation, alterations in RORγt expression were marginal and not statistically significant in our study. Overall, the analysis of transcription factors displays prevalence of Stat1/Stat2/T-bet/Th1 nexus over the other types of T lineage differentiation. In addition to the regulation of T-cell differentiation, multivalent DLL1 in combination with TCR stimulation demonstrated ability to accelerate proliferation of T cells in human PBMC. Thus, stimulation of Notch signaling with multivalent DLL1 could be a potent therapeutically relevant approach to promote anti-tumor Th1 and $CD8^+$ T-cell effector functions via modulation of the expression of transcription factors associated with T-cell differentiation, regulation of Stat signaling, and enhanced T-cell proliferation.

Our results are in agreement with the notion that the Notch system regulates T-cell differentiation and lineage commitment by providing the instructive signals during the induction of antigen-specific responses and with the fact that most gain-of-function experiments suggest that high expression of Delta-like ligands promotes Th1 type responses (6, 7). Although somewhat controversial, strong evidence implicated Notch1 and 2 in the induction of antitumor immunity, including induction of tumor-specific CTL and central memory T cells (5, 43). Together with these data, our results point to the functional axis DLL1/Notch1 and/or Notch2 as an immunotherapeutic target for activation and validate the clinically relevant approach to effectively induce effector T-cell differentiation and T-cell–mediated immunity critical for tumor rejection.

The strong immune stimulatory effect of pharmacologically enhanced DLL1-mediated Notch signaling supports the concept that multivalent DLL1 could be used as a novel immunotherapeutic to induce robust immune responses, provide effective tumor surveillance, and prolong tumor-free survival when combined with tumor oncogene-targeted therapies. In our studies with the erlotinib treatment of the experimental mutant EGFR-dependent lung cancer, the hypothesis was that the correction and stimulation of the host immune system by Notch activation before and during the massive tumor cell killing by EGFR inhibitor would elicit strong effector and memory T-cell responses. This would provide significant clinical benefit by immune-mediated elimination of residual and circulating tumor cells/cancer stem cells and/or by rejection of recurrent tumors via eliciting effective T-cell memory. Indeed, data suggest that stronger immune responses elicited by combination treatment effectuated sustained tumor destruction and extended the PFS.

Growing evidence shows that pleiotropic functions of Notch can be tumor suppressive or oncogenic depending on the cellular context in both solid tumors and hematologic malignancies (44–46). Our data suggest the therapeutic safety of enhancement of DLL1/Notch signaling by systemic administration of the multivalent DLL1 reagent. The experiments with multiple human lung and mouse tumor cells demonstrated that clustered DLL1 increases neither proliferation nor clonogenic potential of cancer cells. *In vivo* studies revealed an antitumor effect of this reagent associated with decreased tumor angiogenesis, improved T-cell differentiation and increased tumor infiltration by T cells and DCs. Implying safety of the enhanced hematopoietic DLL1/Notch signaling was our observation that mice overexpressing DLL1 in bone marrow appeared normal and did not display any behavioral, tissue, or hematopoietic abnormalities (21). In another study, DLL1-mediated signaling was implicated in the inhibition of melanoma growth due to the attenuated vascularization (37). It is also important to note that inactivating Notch mutations are being discovered in cancers, suggesting that the Notch pathway could have an important tumor-suppressor role (47). For therapeutic applications, a short-term regimen of multivalent DLL1 might be sufficient to boost immune system and induce tumor-specific immune responses. Combinations of immune stimulatory multivalent DLL1 with other therapies associated with the release of tumor antigens holds promise to be effective in inducing long-lasting immune responses.

Multiple studies in recent years have called into question the use of Notch inhibitors to treat cancer because of an increased risk of endothelial cell tumors seen in animal models (48). Our studies have shown that downregulation of Notch signaling in the host may promote evasion of the immune system by tumors. Data presented here suggest that, instead of blocking the Notch pathway, ligand-specific and controlled restoration of the Notch signaling would benefit antitumor immunity and provide clinical benefit. These data underscore the novel role of DLL1/Notch, most likely, Notch1 and 2 signaling in the induction of T-cell antitumor immune responses.

Successful application of multivalent DLL1 predicted by our studies opens a venue for exploration of a novel set of therapeutics based on the multivalent forms of Notch ligands for modulation of Notch signaling under various pathologic conditions.

## Disclosure of Potential Conflicts of Interest

D.P. Carbone reports receiving a commercial research grant from Bristol Myers Squibb and is a consultant/advisory board member for Merck, Genentech/Roche, Boehringer Ingelheim, Novartis, and Pfizer. No potential conflicts of interest were disclosed by the other authors.

## Authors' Contributions

**Conception and design:** A.K. Biktasova, D.P. Carbone, A. Shanker, M.M. Dikov
**Development of methodology:** A.K. Biktasova, D.F. Dudimah, K. Park, A. Akhter, S.V. Novitskiy, E.E. Tchekneva, D.P. Carbone, A. Shanker, M.M. Dikov
**Acquisition of data (provided animals, acquired and managed patients, provided facilities, etc.):** A.K. Biktasova, D.F. Dudimah, R.V. Uzhachenko, K. Park, A. Akhter, R.R. Arasada, S.V. Novitskiy, A. Shanker
**Analysis and interpretation of data (e.g., statistical analysis, biostatistics, computational analysis):** A.K. Biktasova, D.F. Dudimah, R.V. Uzhachenko, K. Park, A. Akhter, E.E. Tchekneva, D.P. Carbone, A. Shanker, M.M. Dikov
**Writing, review, and/or revision of the manuscript:** A.K. Biktasova, D.F. Dudimah, R.V. Uzhachenko, K. Park, J.V. Evans, D.P. Carbone, A. Shanker, M.M. Dikov
**Administrative, technical, or material support (i.e., reporting or organizing data, constructing databases):** A.K. Biktasova, K. Park, D.P. Carbone, A. Shanker, M.M. Dikov
**Study supervision:** D.P. Carbone, A. Shanker, M.M. Dikov

## Acknowledgments

The authors thank Elena M. Dikova for editing the article and D. Luke, D. Dulcinea, and Dr. M.C. Thounaojam for their help with the article and figure preparation; they also thank the Vanderbilt University Institute of Imaging Sciences for the assistance with the small animal MRI.

## Grant Support

This work was supported by NIH grants R01CA138923 (M.M. Dikov) and RO1CA175370 (M.M. Dikov and D.P. Carbone), Ohio State University Drug Development Institute grant (M.M. Dikov), Dallapezze Fund (M.M. Dikov and D.P. Carbone), Pilot Project in Lung Cancer SPORE P50CA90949 (M.M. Dikov and A. Shanker), Meharry Clinical and Translational Research Center Pilot Grant U54 MD007593 (A. Shanker), U54 CA163069 (A. Shanker), and SC1 CA182843 (A. Shanker).

The costs of publication of this article were defrayed in part by the payment of page charges. This article must therefore be hereby marked *advertisement* in accordance with 18 U.S.C. Section 1734 solely to indicate this fact.

Received April 17, 2014; revised August 6, 2015; accepted August 12, 2015; published OnlineFirst September 24, 2015.

## References

1. Fiuza UM, Arias AM. Cell and molecular biology of Notch. J Endocrinol 2007;194:459–74.
2. Kopan R, Ilagan MX. The canonical Notch signaling pathway: unfolding the activation mechanism. Cell 2009;137:216–33.
3. Bettelli E, Carrier Y, Gao W, Korn T, Strom TB, Oukka M, et al. Reciprocal developmental pathways for the generation of pathogenic effector TH17 and regulatory T cells. Nature 2006;441:235–8.
4. Maekawa Y, Tsukumo S, Chiba S, Hirai H, Hayashi Y, Okada H, et al. Delta1-Notch3 interactions bias the functional differentiation of activated $CD4^+$ T cells. Immunity 2003;19:549–59.
5. Sierra RA, Thevenot P, Raber PL, Cui Y, Parsons C, Ochoa AC, et al. Rescue of notch-1 signaling in antigen-specific $CD8^+$ T cells overcomes tumor-induced T-cell suppression and enhances immunotherapy in cancer. Cancer Immunol Res 2014;2:800–11.
6. Amsen D, Antov A, Flavell RA. The different faces of Notch in T-helper-cell differentiation. Nat Rev Immunol 2009;9:116–24.
7. Amsen D, Blander JM, Lee GR, Tanigaki K, Honjo T, Flavell RA. Instruction of distinct CD4 T helper cell fates by different notch ligands on antigen-presenting cells. Cell 2004;117:515–26.
8. Tanigaki K, Tsuji M, Yamamoto N, Han H, Tsukada J, Inoue H, et al. Regulation of alphabeta/gammadelta T-cell lineage commitment and peripheral T-cell responses by Notch/RBP-J signaling. Immunity 2004; 20:611–22.
9. Amsen D, Antov A, Jankovic D, Sher FA, Radtke F, Souabni A, et al. Direct regulation of Gata3 expression determines the T helper differentiation potential of Notch. Immunity 2007;27:89–99.
10. Krawczyk CM, Sun J, Pearce EJ. Th2 differentiation is unaffected by Jagged2 expression on dendritic cells. J Immunol 2008;180:7931–7.
11. Ladi E, Nichols JT, Ge W, Miyamoto A, Yao C, Yang LT, et al. The divergent DSL ligand Dll3 does not activate Notch signaling but cell autonomously attenuates signaling induced by other DSL ligands. J Cell Biol 2005; 170:983–92.
12. Skokos D, Nussenzweig MC. CD8-DCs induce IL-12-independent Th1 differentiation through Delta 4 Notch-like ligand in response to bacterial LPS. J Exp Med 2007;204:1525–31.
13. Kassner N, Krueger M, Yagita H, Dzionek A, Hutloff A, Kroczek R, et al. Cutting edge: plasmacytoid dendritic cells induce IL-10 production in T cells via the Delta-like-4/Notch axis. J Immunol 2010;184:550–4.
14. Liotta F, Frosali F, Querci V, Mantei A, Filì L, Maggi L, et al. Human immature myeloid dendritic cells trigger a TH2-polarizing program via Jagged-1/Notch interaction. J Allergy Clin Immunol 2008;121:1000–5 e8.
15. Sun J, Krawczyk CJ, Pearce EJ. Suppression of Th2 cell development by Notch ligands Delta1 and Delta4. J Immunol 2008;180:1655–61.
16. Vigouroux S, Yvon E, Wagner HJ, Biagi E, Dotti G, Sili U, et al. Induction of antigen-specific regulatory T cells following overexpression of a Notch ligand by human B lymphocytes. J Virol 2003;77: 10872–80.
17. Yvon ES, Vigouroux S, Rousseau RF, Biagi E, Amrolia P, Dotti G, et al. Overexpression of the Notch ligand, Jagged-1, induces alloantigen-specific human regulatory T cells. Blood 2003;102:3815–21.
18. Kared H, Adle-Biassette H, Fois E, Masson A, Bach JF, Chatenoud L, et al. Jagged2-expressing hematopoietic progenitors promote regulatory T-cell expansion in the periphery through notch signaling. Immunity 2006;25:823–34.
19. Keerthivasan S, Suleiman R, Lawlor R, Roderick J, Bates T, Minter L, et al. Notch signaling regulates mouse and human Th17 differentiation. J Immunol 2011;187:692–701.
20. Huang Y, Chen X, Dikov MM, Novitskiy SV, Mosse CA, Yang L, et al. Distinct roles of VEGFR-1 and VEGFR-2 in the aberrant hematopoiesis associated with elevated levels of VEGF. Blood 2007; 110:624–31.
21. Huang Y, Lin L, Shanker A, Malhotra A, Yang L, Dikov MM, et al. Resuscitating cancer immunosurveillance: selective stimulation of DLL1-Notch signaling in T cells rescues T-cell function and inhibits tumor growth. Cancer Res 2011;71:6122–31.
22. Novitskiy SV, Csiki I, Huang Y, Johnson DH, Harth EM, Carbone DP, et al. Anti-vascular endothelial growth factor treatment in combination with chemotherapy delays hematopoietic recovery due to decreased proliferation of bone marrow hematopoietic progenitor cells. J Thorac Oncol 2010;5:1410–5.
23. Lee CT, Ciernik IF, Wu S, Tang DC, Chen HL, Truelson JM, et al. Increased immunogenicity of tumors bearing mutant p53 and P1A epitopes after transduction of B7–1 via recombinant adenovirus. Cancer Gene Ther 1996;3:238–44.
24. Politi K, Zakowski MF, Fan PD, Schonfeld EA, Pao W, Varmus HE. Lung adenocarcinomas induced in mice by mutant EGF receptors found in human lung cancers respond to a tyrosine kinase inhibitor or to downregulation of the receptors. Genes Dev 2006;20: 1496–510.
25. Novitskiy SV, Ryzhov S, Zaynagetdinov R, Goldstein AE, Huang Y, Tikhomirov OY, et al. Adenosine receptors in regulation of dendritic cell differentiation and function. Blood 2008;112:1822–31.
26. Heinzel K, Benz C, Bleul CC. A silent chemokine receptor regulates steady-state leukocyte homing *in vivo*. Proc Natl Acad Sci U S A 2007; 104:8421–6.
27. Gabrilovich DI, Ishida T, Nadaf S, Ohm JE, Carbone DP. Antibodies to vascular endothelial growth factor enhance the efficacy of cancer immunotherapy by improving endogenous dendritic cell function. Clin Cancer Res 1999;5:2963–70.
28. Chen JQ, Xiu QY, Shen C, Yan ZM. [Treatment of spontaneous metastatic lung cancer with interleukin-12 gene-modified dendritic cells vaccine]. Ai Zheng 2002;21:1328–31.
29. Mandelboim O, Bar-Haim E, Vadai E, Fridkin M, Eisenbach L. Identification of shared tumor-associated antigen peptides between two spontaneous lung carcinomas. J Immunol 1997;159:6030–6.
30. Ryzhov S, Novitskiy SV, Zaynagetdinov R, Goldstein AE, Carbone DP, Biaggioni I, et al. Host A(2B) adenosine receptors promote carcinoma growth. Neoplasia 2008;10:987–95.
31. Yang XO, Panopoulos AD, Nurieva R, Chang SH, Wang D, Watowich SS, et al. STAT3 regulates cytokine-mediated generation of inflammatory helper T cells. J Biol Chem 2007;282:9358–63.
32. Quigley M, Huang X, Yang Y. STAT1 signaling in CD8 T cells is required for their clonal expansion and memory formation following viral infection *in vivo*. J Immunol 2008;180:2158–64.
33. Feoktistov I, Ryzhov S, Goldstein AE, Biaggioni I. Mast cell-mediated stimulation of angiogenesis: cooperative interaction between A2B and A3 adenosine receptors. Cir Res 2003;92:485–92.
34. Jones CA, Tsukamoto T, O'Brien PC, Uhl CB, Alley MC, Lieber MM. Soft agarose culture human tumour colony forming assay for drug sensitivity testing: [3H]-thymidine incorporation vs. colony counting. Br J Cancer 1985;52:303–10.
35. Heinzel K, Benz C, Martins VC, Haidl ID, Bleul CC. Bone marrow-derived hemopoietic precursors commit to the T-cell lineage only after arrival in the thymic microenvironment. J Immunol 2007;178: 858–68.
36. Jochems C, Schlom J. Tumor-infiltrating immune cells and prognosis: the potential link between conventional cancer therapy and immunity. Exp Biol Med 2011;236:567–79.

37. Zhang JP, Qin HY, Wang L, Liang L, Zhao XC, Cai WX, et al. Overexpression of Notch ligand Dll1 in B16 melanoma cells leads to reduced tumor growth due to attenuated vascularization. Cancer Lett 2011; 309:220–7.
38. Wang Y, Schmid-Bindert G, Zhou C. Erlotinib in the treatment of advanced non–small cell lung cancer: an update for clinicians. Ther Adv Med Oncol 2012;4:19–29.
39. Pao W, Ladanyi M, Miller VA. Erlotinib in lung cancer. N Engl J Med 2005;353:1739–41.
40. Pao W, Miller VA, Politi KA, Riely GJ, Somwar R, Zakowski MF, et al. Acquired resistance of lung adenocarcinomas to gefitinib or erlotinib is associated with a second mutation in the EGFR kinase domain. PLoS Med 2005;2:e73.
41. Gale NW, Dominguez MG, Noguera I, Pan L, Hughes V, Valenzuela DM, et al. Haploinsufficiency of delta-like 4 ligand results in embryonic lethality due to major defects in arterial and vascular development. Proc Natl Acad Sci U S A 2004;101:15949–54.
42. Delaney C, Varnum-Finney B, Aoyama K, Brashem-Stein C, Bernstein ID. Dose-dependent effects of the Notch ligand Delta1 on *ex vivo* differentiation and *in vivo* marrow repopulating ability of cord blood cells. Blood 2005;106:2693–9.
43. Sugimoto K, Maekawa Y, Kitamura A, Nishida J, Koyanagi A, Yagita H, et al. Notch2 signaling is required for potent antitumor immunity *in vivo*. J Immunol 2010;184:4673–8.
44. Lobry C, Oh P, Aifantis I. Oncogenic and tumor suppressor functions of Notch in cancer: it's NOTCH what you think. J Exp Med 2011;208:1931–5.
45. Klinakis A, Lobry C, Abdel-Wahab O, Oh P, Haeno H, Buonamici S, et al. A novel tumour-suppressor function for the Notch pathway in myeloid leukaemia. Nature 2011;473:230–3.
46. Roodhart JM, He H, Daenen LG, Monvoisin A, Barber CL, van Amersfoort M, et al. Notch1 regulates angio-supportive bone marrow-derived cells: relevance to chemoresistance. Blood 2013;122:143–53.
47. Stransky N, Egloff AM, Tward AD, Kostic AD, Cibulskis K, Sivachenko A, et al. The mutational landscape of head and neck squamous cell carcinoma. Science 2011;333:1157–60.
48. Yan M, Callahan CA, Beyer JC, Allamneni KP, Zhang G, Ridgway JB, et al. Chronic DLL4 blockade induces vascular neoplasms. Nature 2010;463:E6–7.